Supplementary Materials

Figure S1. Characterization of the double-network hydrogel properties.

Figure S2. Scanning electron microscopy (SEM) images of the double-network hydrogel.

Figure S3. Adhesive properties of PAM-PVA_{10} hydrogel.

Figure S4. The output performance of the SH-TENG.

Figure S5. The screenshots and photos of the self-powered raindrops visual sensing system.

Figure S6. The screenshots of the raindrop monitoring.

Video S1. SH-TENG drives 50 LEDs.

Video S2. Hydrogel as electrode to achieve stretchable luminescence.

Video S3. The system monitors the raindrop and luminous display.

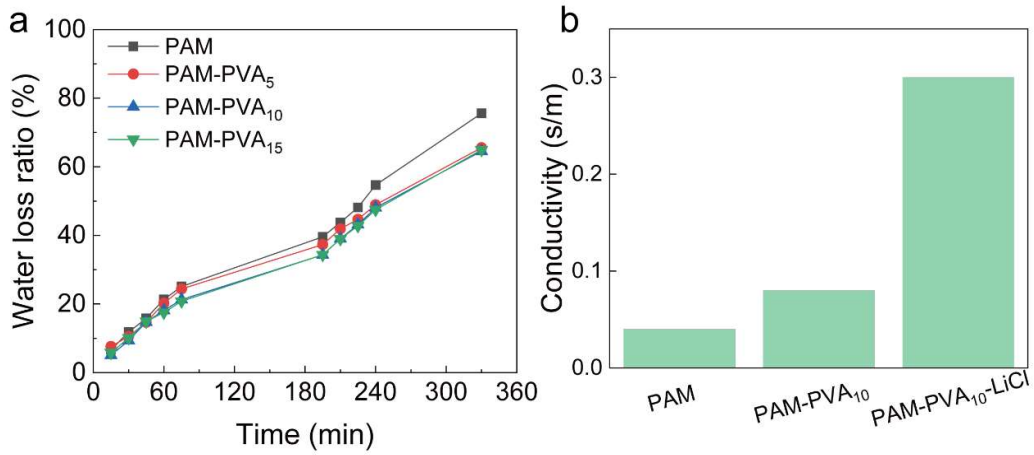

Figure S1. Characterization of double-network hydrogel properties. (a) Water loss ratio of hydrogel. (b) Conductivity of hydrogels with various components.

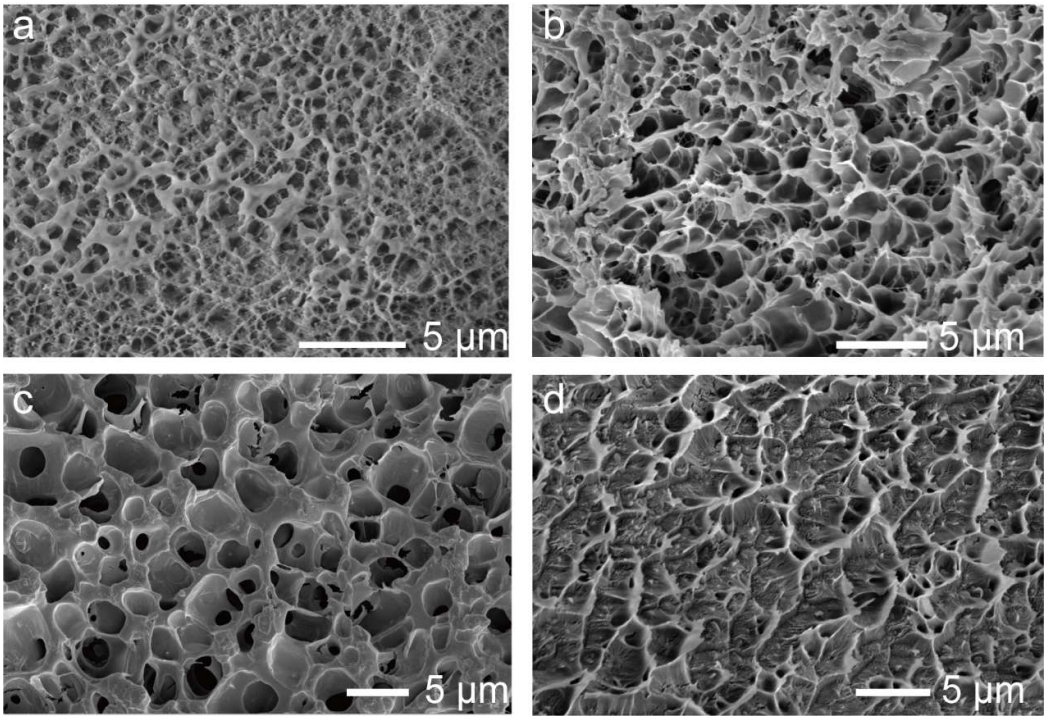

Figure S2. Scanning electron microscopy (SEM) images of the double-network hydrogel. SEM of (a) PAM, (b) PAM-PVA_5, (c) PAM-PVA_{10} and (d) PAM-PVA_{15} hydrogel, respectively.

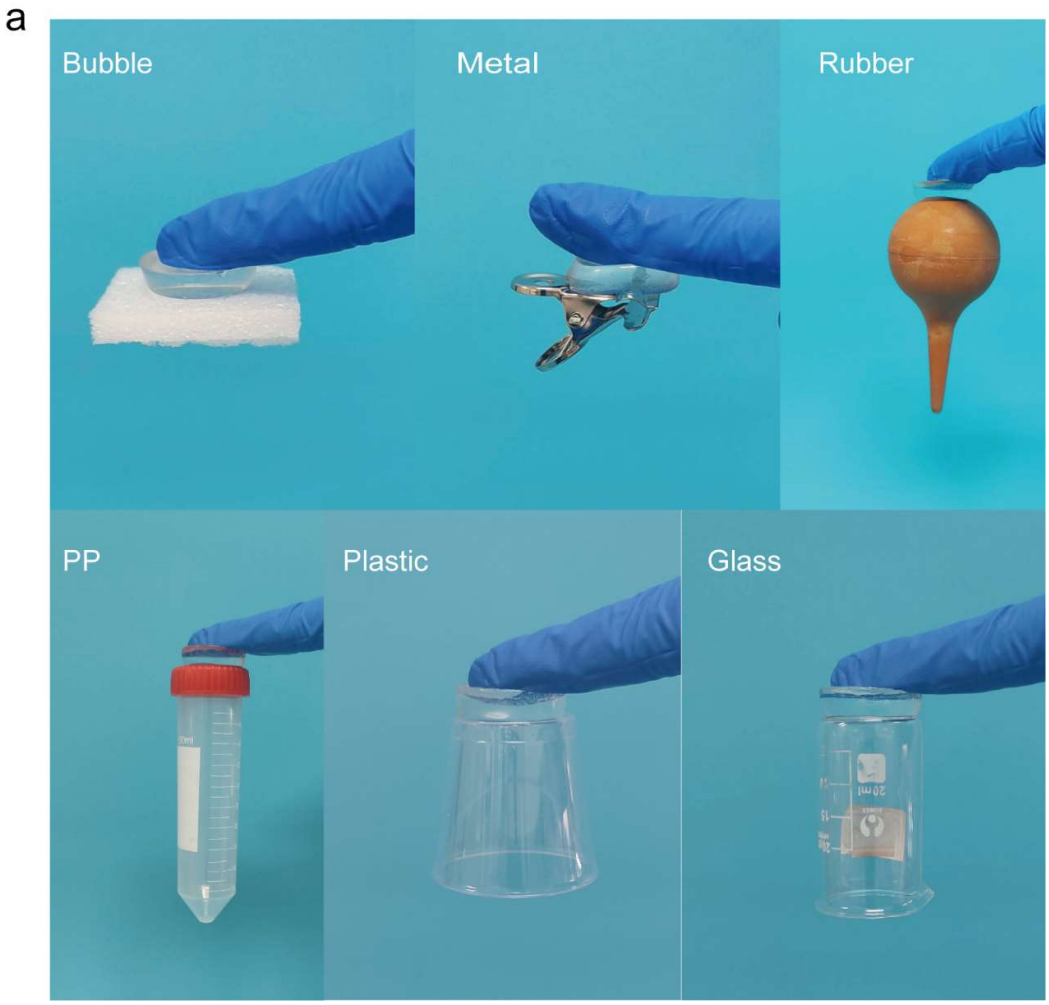

Figure S3. Adhesive properties of PAM-PVA$_{10}$ hydrogel. (a) The PAM-PVA$_{10}$ hydrogel adheres to a variety of materials, including bubble, metal, rubber, PP, plastic, and glass.

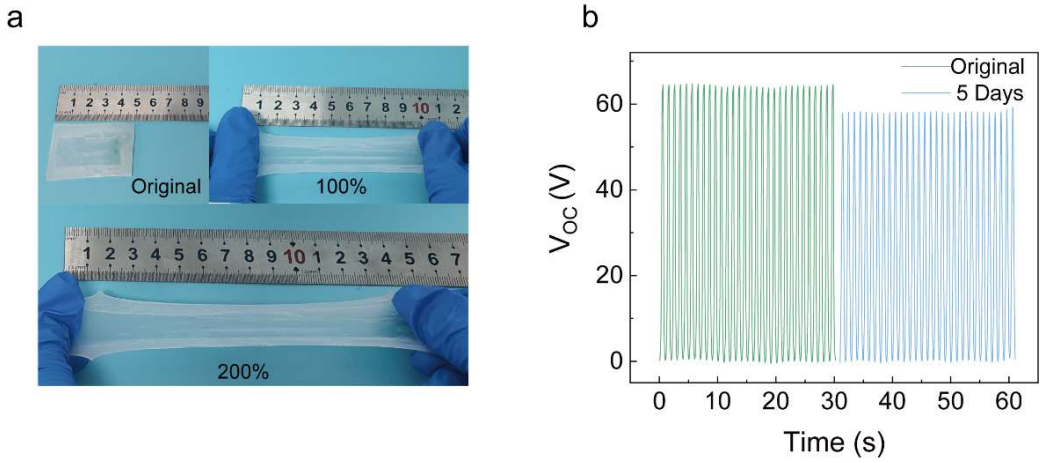

Figure S4. The performance of the SH-TENG. (a) Tensile properties of SH-TENG. (b) Electrical properties of PAM-PVA_{10} hydrogel after 5 days at room temperature.

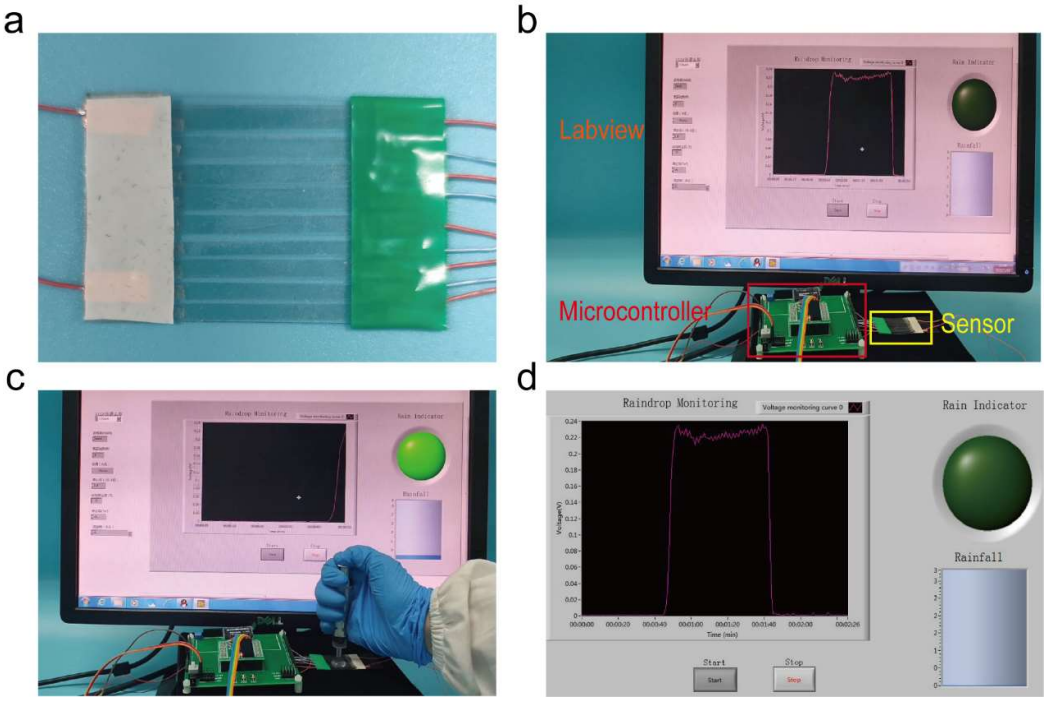

Figure S5. The screenshots and photos of the self-powered raindrops visual sensing system. (a) Photograph of the self-powered raindrops visual sensor. (b) Photograph of the experimental setup of the self-powered raindrops visual sensing system. (c) Optical image of raindrop falling on the sensor. (d) Screenshot of the self-powered raindrops visual sensing system during the test.

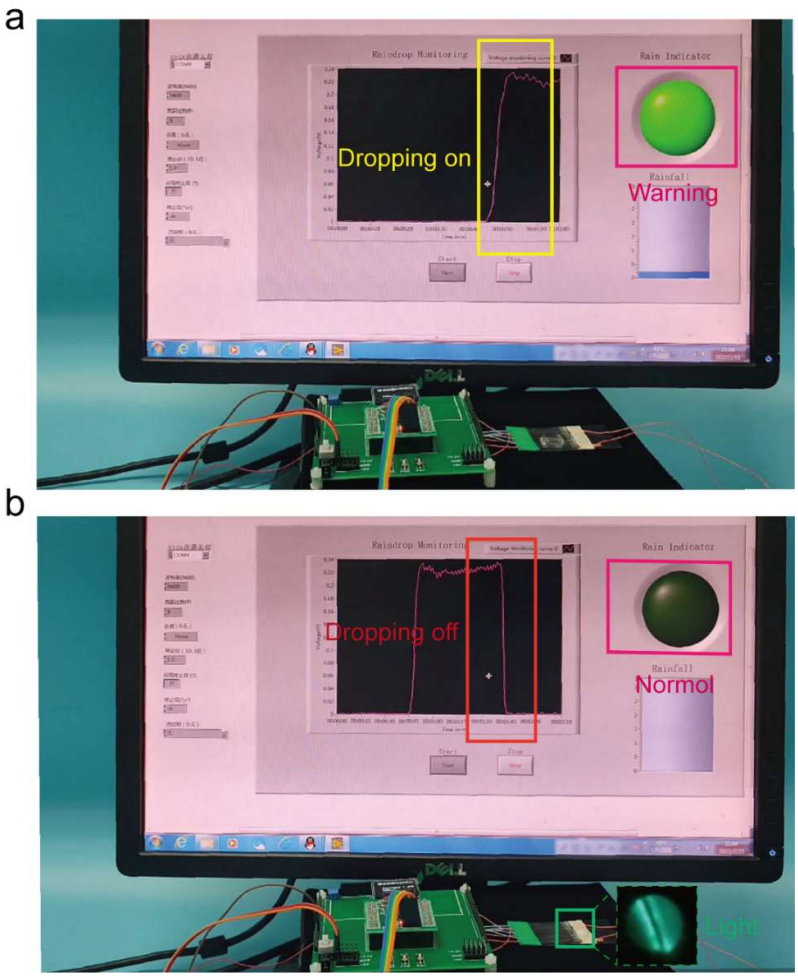

Figure S6. The screenshots of the raindrop monitoring. (a) Warning in case of raindrops.

(b) Monitoring without raindrops and luminous display.